Anal. Chem. **2010,** *82,* 7351–7356

Quantum Dots Based Electrochemiluminescent Immunosensor by Coupling Enzymatic Amplification with Self-Produced Coreactant from Oxygen Reduction

Xuan Liu, Yangyang Zhang, Jianping Lei, Yadong Xue, Lingxiao Cheng, and Huangxian Ju*

Key Laboratory of Analytical Chemistry for Life Science (Ministry of Education of China), and Department of Chemistry, Nanjing University, Nanjing 210093, P. R. China

A highly sensitive competitive immunosensor based on the electrochemiluminescence (ECL) of quantum dots (QDs) was proposed by coupling with an enzymatic amplification. The fabrication process of the immunosensor was traced with atomic force microscopic images and electrochemical impedance spectra. The strong cathodic ECL emission of the immobilized QDs could be detected at a relatively low emission potential. The reduction of dissolved oxygen during the cathodic process provided a self-produced coreactant, H_2O_2, for the ECL emission. Using human IgG (HIgG) as a model protein, upon the immuno-recognition of the immobilized HIgG to its antibody labeled simply with horseradish peroxidase, the ECL intensity decreased due to the steric hindrance of the proteins to electron transfer. The decrease could be greatly amplified by an enzymatic cycle to consume the self-produced coreactant, leading to a wide calibration range of 0.05 ng mL^{-1} ∼ 5 μg mL^{-1} and a low limit of detection for the competitive immunoassay of HIgG. This immunosensor showed good stability and fabrication reproducibility. The immunoassays of practical samples showed acceptable results. This facile immunosensing strategy opened a new avenue for detection of proteins and application of QDs in ECL biosensing.

Semiconductor nanocrystal or quantum dots (QDs) have been widely used as optical[1] or electric[2] labels in bioanalysis due to their significant advantages of size-control photoluminescence (PL), good stability against photobleaching and subsequent chemical solubilization to release electrochemical detectable ions for sensitive quantitative readout.[3] Since silica-coated core (CdSe)-shell (ZnS or CdS) QDs with biocompatibility were reported in 1998,[4] the functionalization of various QDs with multitudinous biomolecules has attracted considerable interest in fundamental research and practical application, such as cellular imaging,[5] monitoring of specific biorecognition[6−8] and structurally induced biomolecular transformations,[9,10] DNA hybridization analysis,[11] immunoassay,[2,12] detection of cell surface carbohydrates,[13] and clinical diagnosis.[14] The electrochemiluminescence (ECL) of QDs has also extensively used for biosensing since the first ECL sensor was proposed using CdSe QDs as ECL emitter in 2004.[15] Especially, II−VI QDs, such as CdS, CdSe, and CdTe QDs, have become the most popular ECL emitters of QDs in aqueous systems.[16−22] In order to enhance ECL intensity, many compounds, such as H_2O_2,[15,16] $S_2O_8^{2-}$,[17] SO_3^{2-},[19] and amines,[22] have been employed as the cathodic or anodic ECL coreactants of QDs. These extrinsic coreactants can generally react with QDs to produce hole-injected[15−17] or electron-injected[19] QDs for cathodic or anodic ECL emission. However, they are difficult to further couple with other signal amplification processes for highly sensitive biosensing. This work made use of the cathodic ECL

* To whom correspondence should be addressed. Phone/Fax: +86-25-83593593. E-mail: hxju@nju.edu.cn.

(1) Bruns, O. T.; Ittrich, H.; Peldschus, K.; Kaul, M. G.; Tromsdorf, U. I.; Lauterwasser, J.; Nikolic, M. S.; Mollwitz, B.; Merkel, M.; Bigall, N. C.; Sapra, S.; Reimer, R.; Hohenberg, H.; Weller, H.; Eychmüller, A.; Adam, G.; Beisiegel, U.; Heeren, J. *Nat. Nanotechnol.* **2009**, *4*, 193–201.
(2) Liu, G. D.; Wang, J.; Kim, J.; Jan, M. R. *Anal. Chem.* **2004**, *76*, 7126–7130.
(3) Gill, R.; Zayats, M.; Willner, I. *Angew. Chem., Int. Ed.* **2008**, *47*, 7602–7625.
(4) Bruchez, M., Jr.; Moronne, M.; Gin, P.; Weiss, S.; Alivisatos, A. P. *Science* **1998**, *281*, 2013–2016.
(5) Michalet, X.; Pinaud, F. F.; Bentolila, L. A.; Tsay, J. M.; Doose, S.; Li, J. J.; Sundaresan, G.; Wu, A. M.; Gambhir, S. S.; Weiss, S. *Science* **2005**, *307*, 538–544.
(6) Liu, J. W.; Lee, J. H.; Lu, Y. *Anal. Chem.* **2007**, *79*, 4120–4125.
(7) Yuan, J. P.; Guo, W. W.; Wang, E. K. *Anal. Chem.* **2008**, *80*, 1141–1145.
(8) Mukundan, H.; Xie, H. Z.; Price, D.; Kubicek-Sutherland, J. Z.; Grace, W. K.; Anderson, A. S.; Martinez, J. S.; Hartman, N.; Swanson, B. I. *Anal. Chem.* **2010**, *82*, 136–144.
(9) Freeman, R.; Gill, R.; Shweky, I.; Kotler, M.; Banin, U.; Willner, I. *Angew. Chem., Int. Ed.* **2009**, *48*, 309–313.
(10) Peng, H.; Zhang, L. J.; Kjällman, T. H. M.; Soeller, C.; Travas-Sejdic, J. *J. Am. Chem. Soc.* **2007**, *129*, 3048–3049.
(11) Wang, J.; Liu, G.; Merkoci, A. *J. Am. Chem. Soc.* **2003**, *125*, 3214–3215.
(12) Liu, G. D.; Wang, J.; Barry, R.; Petersen, C.; Timchalk, C.; Gassman, P. L.; Lin, Y. H. *Chem.—Eur. J.* **2008**, *14*, 9951–9959.
(13) Ding, L.; Cheng, W.; Wang, X. J.; Ding, S. J.; Ju, H. X. *J. Am. Chem. Soc.* **2008**, *130*, 7224–7225.
(14) Choi, H. S.; Liu, W. H.; Liu, F. B.; Nasr, K.; Misra, P.; Bawendi, M. G.; Frangioni, J. V. *Nat. Nanotechnol.* **2010**, *5*, 42–47.
(15) Zou, G. Z.; Ju, H. X. *Anal. Chem.* **2004**, *76*, 6871–6876.
(16) Wang, X. F.; Zhou, Y.; Xu, J. J.; Chen, H. Y. *Adv. Funct. Mater.* **2009**, *19*, 1444–1450.
(17) Jie, G. F.; Liu, B.; Pan, H. C.; Zhu, J. J.; Chen, H. Y. *Anal. Chem.* **2007**, *79*, 5574–5581.
(18) Liu, X.; Jiang, H.; Lei, J. P.; Ju, H. X. *Anal. Chem.* **2007**, *79*, 8055–8060.
(19) Liu, X.; Ju, H. X. *Anal. Chem.* **2008**, *80*, 5377–5382.
(20) Shan, Y.; Xu, J. J.; Chen, H. Y. *Chem. Commun.* **2009**, 905–907.
(21) Cheng, L. X.; Liu, X.; Lei, J. P.; Ju, H. X. *Anal. Chem.* **2010**, *82*, 3359–3364.
(22) Zhang, L. H.; Zou, X. Q.; Ying, E. B.; Dong, S. J. *J. Phys. Chem. C* **2008**, *112*, 4451–4454.

10.1021/ac1013942
Published on Web 08/09/2010

Scheme 1. Construction (A) and Incubation (B) of the Immunosensor, and ECL Detection without (C) and with (D, E) the Enzymatic Amplification by Consumption of H_2O_2 as Coreactant

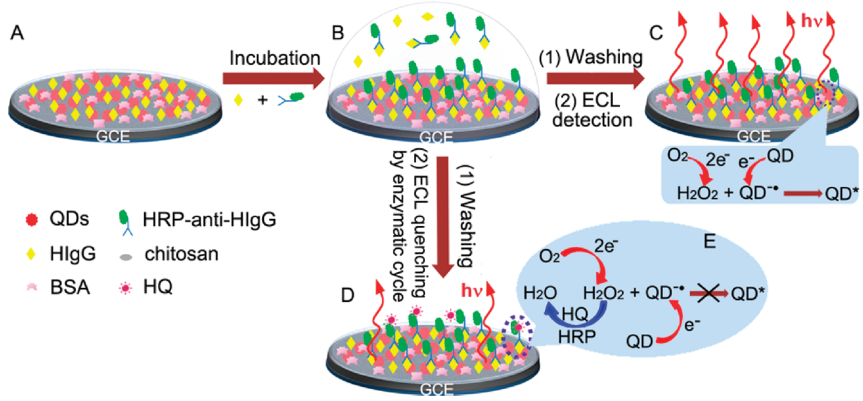

emission process of surface unpassivated CdTe QDs at relatively low potential,[21] in which H_2O_2 acted as a self-produced coreactant, to propose an enzymatic amplification for convenient, rapid and highly sensitive ECL immunosensing.

Owing to the advantages of electrochemical detection and the highly specific recognition between antibody and antigen, electrochemical immunosensors have been quickly developed[23,24] for competitive,[25] sandwich-type,[26−28] and separation-free[29] immunoassay of proteins in ng mL^{-1} to hundreds of ng mL^{-1} level. The sensitivity of sandwich-type immunoassay can be further improved by using metal or silica nanoparticles, nanotubes or other nano/micromaterials as carriers of antibody and enzyme.[30−33] Although the preparation of the antibody and enzyme functionalized nano/micromaterials is relatively complex, the high loading of enzyme for each immuno-recognition greatly amplifies the detection signal.[31−33] Another signal amplification strategy for immunoassay is the application of stripping voltammetry coupled with a preconcentration step for measuring metal ions.[34] The metal ions are released from each metal nanoparticle or QD.[2,35] A sensitive immunoassay for IgG down to 3 pM (0.45 ng mL^{-1}) has been proposed by using gold nanoparticles to label the antibody.[35] However, these signal amplification strategies have not been applied in QD-based ECL immunoassay, though the mercaptoacetic acid capped CdSe QD-based ECL immunosensing has been developed.[36] The main limitation includes two factors. First, the ECL emission cannot be combined with a stripping voltammetric measurement. And the second, different from the enzymatic-catalyzed electrochemical immunoassay, few QD-based ECL processes involve the enzymatic cycle.[16,19] This work introduced an enzymatic cycle to a H_2O_2-generated ECL process of QDs for amplifying the detection signal. The resulting ECL immunosensing method could avoid any complex labeling process.

The immunosensor was constructed by immobilizing meso-2,3-dimercaptosuccinic acid (DMSA)-stabilized CdTe QDs and human IgG (HIgG) as antigen on an electrode surface (Scheme 1). The competitive immuno-recognition of the immobilized HIgG and analyte HIgG to horseradish peroxidase (HRP)-labeled antibody produced a HRP-immobilized surface. In the absence of substrate hydroquinone (HQ), the immobilized QDs could produce an ECL emission through the reaction of the self-produced coreactant H_2O_2 with reduced QDs, while the ECL emission would be quenched in the presence of HQ due to the consumption of H_2O_2 in the HRP-catalyzed oxidation process of HQ.[37,38] The enzymatic cycle amplified the signal change corresponding to the immuno-recognition and led to high sensitivity and wide detection range. The limit of detection was even one-order of magnitude lower than that of nanoparticle-based stripping voltammetric amplification,[35] whereas the detection range was also much wider than those of general competitive electrochemical immunosensors.[39] This work provided a new avenue for signal amplification of ECL biosensing and would extend the application field of QDs in bioanalysis.

EXPERIMENTAL SECTION

Reagents. Cadmium chloride ($CdCl_2 \cdot 2.5H_2O$), DMSA, HQ and 25% glutaraldehyde aqueous solution were purchased from Alfa Aesar China Ltd.. HIgG, HRP labeled anti-HIgG (HRP-anti-HIgG) and bovine serum albumin (BSA) were purchased from Boster Bioengineering Ltd. Co. (China). Chitosan (from crab shells) and tris-base (reagent grade) were purchased from Sigma Chemical Co. (St. Louis, MO). Other reagents were of analytical grade and used as received. The pH of 0.1 M tris-HCl buffer containing 0.1 M KNO_3 was adjusted by adding 1 M HCl. 0.01 M pH 7.4 phosphate buffer solution (PBS) was prepared using K_2HPO_4 and KH_2PO_4. The clinical serum

(23) Li, X. M.; Yang, X. Y.; Zhang, S. S. *TrAC, Trends Anal. Chem.* **2008**, *27*, 543–553.
(24) Wang, J. *Biosens. Bioelectron.* **2006**, *21*, 1887–1892.
(25) Wu, J.; Yan, F.; Tang, J. H.; Zhai, C.; Ju, H. X. *Clin. Chem.* **2007**, *53*, 1495–1502.
(26) Kang, H. J.; Aziz, M. A.; Jeon, B.; Jo, K.; Yang, H. *Electroanalysis* **2009**, *21*, 2647–2652.
(27) Wilson, M. S.; Nie, W. Y. *Anal. Chem.* **2006**, *78*, 2507–2513.
(28) Wilson, M. S. *Anal. Chem.* **2005**, *77*, 1496–1502.
(29) Dai, Z.; Yan, F.; Yu, H.; Hu, X. Y.; Ju, H. X. *J. Immunol. Methods* **2004**, *287*, 13–20.
(30) Zhang, H. Q.; Zhao, Q.; Li, X. F.; Le, X. C. *Analyst* **2007**, *132*, 724–737.
(31) Wu, Y. F.; Chen, C. L.; Liu, S. Q. *Anal. Chem.* **2009**, *81*, 1600–1607.
(32) Tang, D. P.; Ren, J. *J. Anal. Chem.* **2008**, *80*, 8064–8070.
(33) Lai, G. S.; Yan, F.; Ju, H. X. *Anal. Chem.* **2009**, *81*, 9730–9736.
(34) Wang, J. *Analyst* **2005**, *130*, 421–426.
(35) Dequaire, M.; Degrand, C.; Limoges, B. *Anal. Chem.* **2000**, *72*, 5521–5528.
(36) Jie, G. F.; Huang, H. P.; Sun, X. L.; Zhu, J. J. *Biosens. Bioelectron.* **2008**, *23*, 1896–1899.
(37) Chikkaveeraiah, B. V.; Bhirde, A.; Malhotra, R.; Patel, V.; Gutkind, J. S.; Rusling, J. F. *Anal. Chem.* **2009**, *81*, 9129–9134.
(38) Malhotra, R.; Patel, V.; Vaqué, J. P.; Gutkind, J. S.; Rusling, J. F. *Anal. Chem.* **2010**, *82*, 3118–3123.
(39) Wu, J.; Tang, J. H.; Dai, Z.; Yan, F.; Ju, H. X.; El Murr, N. *Biosens. Bioelectron.* **2006**, *22*, 102–108.

samples were from Gulou Hospital (Nanjing, China). The ultrapure water (≥18 MΩ, Milli-Q, Millipore) was used throughout the experiments.

Apparatus. The electrochemical and ECL measurements were carried out on an MPI-E multifunctional electrochemical and chemiluminescent analytical system (Xi'an Remex Analytical Instrument Ltd. Co., China) at room temperature with a configuration consisted of a glassy carbon electrode (GCE, 5.0 mm in diameter, China) as working, a platinum wire as counter, and a Ag/AgCl (saturated KCl solution) as reference electrodes. During measurements, cathodic potential with a range from 0 to −1.0 V was applied to the GCE by cyclic voltammetric (CV) technique, while the ECL emission was recorded. The ECL emission intensity was detected at −0.96 V (vs Ag/AgCl). The emission window was placed in front of the photomultiplier tube (PMT, detection range from 300 to 650 nm) biased at −800 V.

PL experiment was performed on a RF-5301 PC fluorometer (Shimadzu Co., Japan). The UV−vis absorption spectrum was obtained on Shimadzu UV-3600 UV−vis-NIR photospectrometer (Shimadzu Co., Japan). The electrochemical impedance spectra (EIS) were carried out on a PGSTAT30/FRA2 system (Autolab, Netherlands). The atomic force microscopic (AFM) images were obtained from Molecular Imaging Pico SPM (U.S.). As control, the concentrations of IgG in clinical human serum samples were obtained from the Hitachi automatic biochemical analyzer (Japan).

Preparation of DMSA-CdTe QDs. The synthesis of DMSA-CdTe QDs was referred to a green one-pot method reported previously.[40] Briefly, the electrogenerated Te precursor was produced on a CHI 660B workstation (Austin, TX) using Te electrode as a working electrode at −1.0 V (vs Ag/AgCl) in the electrolyte containing 0.6 mM Cd^{2+} and 1.6 mM DMSA as stabilizer under N_2 atmosphere. After electrolysis for 0.5 C, the solution was refluxed at 80 °C for 20 h to obtain the QDs. The as-synthesized QDs could be stable for more than 2 months when kept in a refrigerator at 4 °C.

Construction of Immunosensor. First, 150 μL of the as-prepared QD solution was mixed with 150 μL of isopropyl alcohol and centrifuged at 6000 rmp/min for 3 min. The precipitation was twice washed using 1:1 (*V*/*V*) mixture of water and isopropyl alcohol, and dissolved in 20 μL ultra pure water, which was then dropped on a polished GCE. After dried in air, 10 μL of 0.025% chitosan solution was coated on the QD film for covalent binding of HIgG by activating the chitosan film with 15 μL of 2% glutaraldehyde (in 0.1 M PBS, pH 7.4) for 2 h and incubating 20 μL of HIgG (50 μg mL^{-1} in 0.01 M PBS, pH 7.4) for 60 min at room temperature and overnight at 4 °C. The resulting surface was slowly washed with streams of 0.01% Tween and 0.01 M pH 7.4 PBS, and blocked with 20 μL of 5% BSA solution for 1 h at room temperature to obtain the immunosensor, which was named as GCE/QDs/chitosan-HIgG.

Assay Procedure. Ten μL of HIgG solutions with different concentrations were mixed with 10 μL of 20 μg mL^{-1} HRP-anti-HIgG to obtain the incubation solutions. As shown in Scheme 1B, 20 μL of incubation solution was dropped on the GCE/QDs/chitosan-HIgG and incubated at 37 °C for 45 min, during which the HIgG in the incubation solution competed with the immobilized HIgG to react with the limited binding sites of the HRP-anti-HIgG to form the immunocomplex. After washed with 0.01 M PBS 7.4, the ECL intensity of the resulting GCE/QDs/chitosan-HIgG/HRP-anti-HIgG in 0.1 M pH 9.0 tris-HCl buffer in presence of 0.1 mM HQ was recorded to produce the detection signal corresponding to the analyte (Scheme 1D).

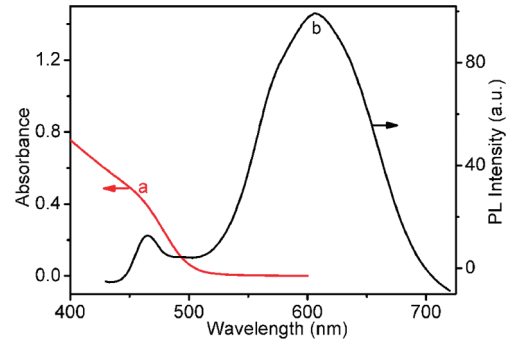

Figure 1. UV−vis (a) and PL (λ_{ex}: 400 nm) (b) spectra of the as-prepared CdTe QDs.

RESULTS AND DISCUSSION

Characterization of DMSA-CdTe QDs. The UV−vis spectrum of the as-prepared DMSA-CdTe QDs showed a wide absorption band with an absorption inflection point at 458 nm (Figure 1, curve a). The PL spectrum of the as-prepared QDs showed a strong emission peak at 607 nm and a weak emission at 465 nm (Figure 1, curve b). The wavelength of the weak emission peak was consistent with the UV−vis absorption inflection point, indicating the band gap emission of the core.[41] Meanwhile, the strong emission peak at the longer wavelength could be attributed to the surface trap emission, which usually shows significantly red shift by hundreds of nanometers compared to the PL emission from the core.[41,42] The emission peak from surface trap at 607 nm suggested lower energy, i.e. narrower band gap of the surface trap than that of the core, leading to a possibility to produce ECL emission at a relatively low potential.[43]

AFM and EIS Characterization of Immunosensor. The AFM image of QDs/chitosan film on a glass substrate showed an undulate height less than 45 nm (Figure 2A). After HIgG was covalently bound to the chitosan surface, the height became 68 nm, and the aggregation of some HIgG molecules could be observed (Figure 2B). After blocked with BSA, the surface morphology showed much more coverage of protein than that before blocking, whereas the undulate height became 100 nm (Figure 2C), indicating that BSA effectively blocked the residue area of the chitosan film. After immunoreaction, the height increased by 15 nm (Figure 2D). The different surface morphology from that before immunoreaction confirmed the specific conjugation of HRP-anti-HIgG to the covalently immobilized HIgG.

The EIS of the resulting electrodes could give further information on the modification process (Figure 3). In EIS, the diameter of semicircle equals to the electron-transfer resistance, R_{et}. The

(40) Ge, C. W.; Xu, M.; Liu, J.; Lei, J. P.; Ju, H. X. *Chem. Commun.* **2008**, 450–452.
(41) Iwasaki, K.; Torimoto, T.; Shibayama, T.; Takahashi, H.; Ohtani, B. *J. Phys. Chem. B* **2004**, *108*, 11946–11952.
(42) Ding, Z. F.; Quinn, B. M.; Haram, S. K.; Pell, L. E.; Korgel, B. A.; Bard, A. J. *Science* **2002**, *296*, 1293–1297.
(43) Poznyak, S. K.; Osipovich, N. P.; Shavel, A.; Talapin, D. V.; Gao, M. Y.; Eychmüller, A.; Gaponik, N. *J. Phys. Chem. B* **2005**, *109*, 1094–1100.

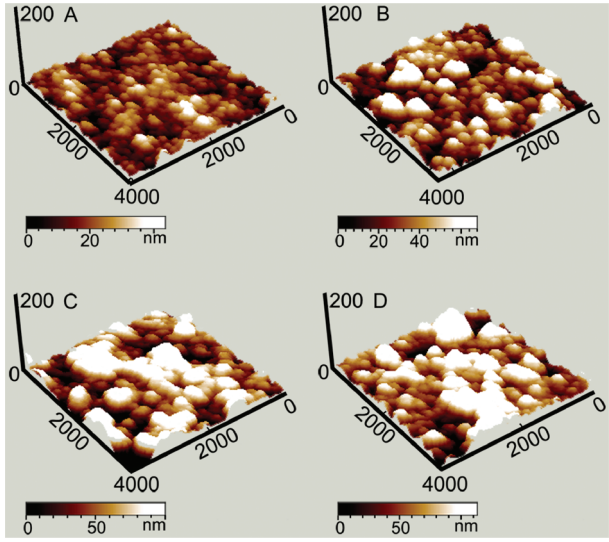

Figure 2. AFM images of QDs/chitosan (A), QDs/chitosan-HIgG before (B) and after (C) blocking with BSA, and QDs/chitosan-HIgG/HRP-anti-HIgG (D).

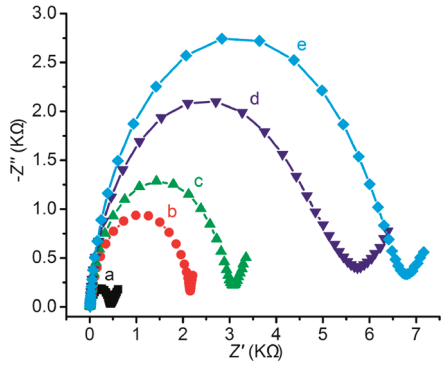

Figure 3. EIS of bare GCE (a), GCE/QDs (b), GCE/QDs/chitosan (c), and GCE/QDs/chitosan-HIgG before (d) and after (e) blocking with BSA in 0.1 M KCl containing 5 mM $[Fe(CN)_6]^{3-}$ and 5 mM $[Fe(CN)_6]^{4-}$.

bare GCE showed a relatively small R_{et} (curve a). After the GCE was coated by QDs, the semiconductor film increased the impedance, thus showed larger R_{et} (curve b). Similarly, chitosan, HIgG and BSA could all resist the electron-transfer kinetics of the redox probe at the electrode interface, resulting in the increasing impedance of the electrode (curves c–e), which testified the immobilization of these substances.

ECL Emission of Immunosensor. The GCE/QDs/chitosan showed a strong cathodic ECL emission in air-saturated pH 9.0 tris-HCl buffer, with an emission peak at −0.87 V, as reported in our previous work,[21] showing a relatively low emission potential. The ECL intensity increased with the increasing pH, which was a character of H_2O_2-generated QD ECL emission, similar to that of CdSe QDs in PBS solution.[44] The H_2O_2 could be produced as a coreactant from the electrochemical reduction of dissolved oxygen at electrode surface.[21]

In air-saturated pH 9.0 tris-HCl buffer, the cyclic voltammogram of GCE/QDs/chitosan-HIgG/HRP-anti-HIgG showed two reduction peaks at −0.66 and −0.80 V, which could be attributed to the reduction of dissolved oxygen and DMSA-CdTe QDs, respectively (Figure 4). The reduction product of dissolved oxygen at −0.66 V was H_2O_2,[45] a common coreactant for QD ECL emission,[15,16,44] leading to an intensive ECL emission peaked at −0.96 V. The more negative ECL emission potential of GCE/QDs/chitosan-HIgG/HRP-anti-HIgG than GCE/QDs/chitosan resulted from the increased impedance, which also resulted in the slight decrease of ECL emission of the immobilized QDs (discussed below). During the cathodic potential scan, the H_2O_2 reacted with the electron-injected $QD^{-\bullet}$ formed at −0.80 V to produce excited QDs, and then ECL emission was observed. The ECL processes could be expressed as follows (Scheme 1D):

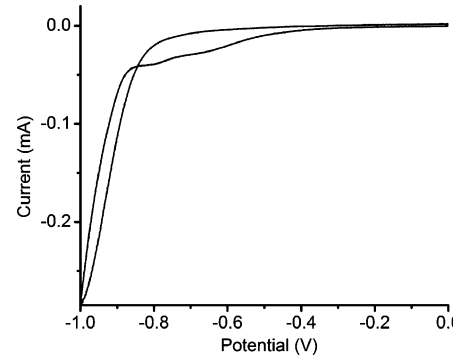

Figure 4. CV curve of GCE/QDs/chitosan-HIgG/HRP-anti-HIgG in air-saturated pH 9.0 tris-HCl buffer containing 0.1 M KNO_3. Scan rate: 0.1 V s^{-1}.

$$CdTe/DMSA + e^- \rightarrow CdTe/DMSA^{-\bullet} \quad (1)$$

$$O_2 + 2e^- + 2H_2O \rightarrow H_2O_2 + 2OH^- \quad (2)$$

$$2CdTe/DMSA^{-\bullet} + H_2O_2 \rightarrow 2OH^- + 2CdTe/DMSA^* \quad (3)$$

$$CdTe/DMSA^* \rightarrow CdTe/DMSA + h\nu \quad (4)$$

In presence of the enzymatic substrate, HQ, the enzymatic reaction could consume H_2O_2 (eq 5), thus resulting in a quenching effect (Scheme 1E). Although H_2O_2 was generated at the electrode surface, the good permeability of chitosan film allowed the proximity of H_2O_2 to both QDs and HRP. During the potential scan H_2O_2 was first produced at −0.66 V, and then consumed via eq 5 in presence of HQ. The product quinone could be verified from the voltammogram (not shown), which showed a new reduction peak at −0.080 V. Although a high pH was favorable to the ECL emission, considering the bioactivity of both immunoreagents and HRP, air-saturated pH 9.0 tris-HCl buffer in presence of 0.1 M KNO_3 and 0.1 mM HQ was used as the detection solution.

$$HQ + H_2O_2 \xrightarrow{HRP} Quinone + H_2O \quad (5)$$

Optimization of Immunoreaction Conditions. The detection sensitivity of the immunosensor depended on the formation of the immunocomplex on the electrode surface, which affected the

(44) Jiang, H.; Ju, H. X. *Anal. Chem.* **2007**, *79*, 6690–6696.

(45) Fang, Y. M.; Sun, J. J.; Wu, A. H.; Su, X. L.; Chen, G. N. *Langmuir* **2009**, *25*, 555–560.

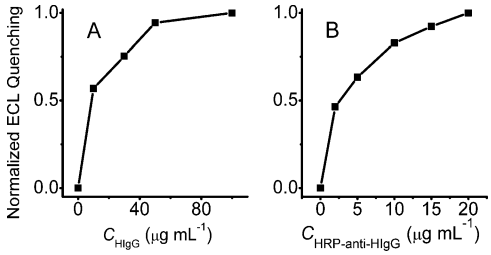

Figure 5. Optimization of concentrations of HIgG (A) and HRP-anti-HIgG (B) for immunosensor construction. The ECL emission was detected in air-saturated pH 9.0 tris-HCl buffer containing 0.1 M KNO_3 and 0.1 mM HQ.

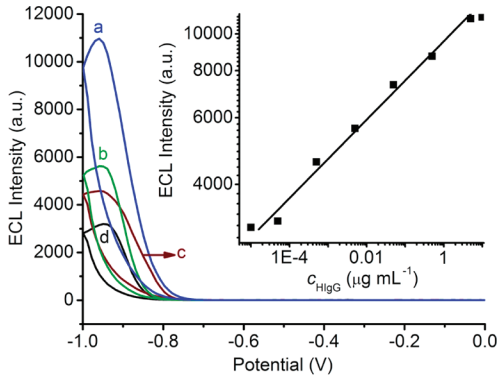

Figure 6. Cyclic ECL curves of GCE/QDs/chitosan-HIgG/HRP-anti-HIgG for HIgG detection at 5 μg mL^{-1} (a), 5 ng mL^{-1} (b), 0.5 ng mL^{-1} (c), and 0.05 ng mL^{-1} (d) in air-saturated detection solution containing 0.1 mM HQ. Inset: linear calibration plot for HIgG detection.

quenching efficiency and was decided by the amount of HIgG (antigen) immobilized on the electrode surface and the concentration of HRP-anti-HIgG (antibody) in the incubation solution (Figure 5). Twenty μL of 10 μg mL^{-1} HRP-anti-HIgG was used as the incubation solution to obtain the optimal amount of HIgG. The quenching response of GCE/QDs/chitosan-HIgG/HRP-anti-HIgG showed a platform when the concentration of HIgG used for immunosensor preparation was beyond 50 μg mL^{-1}, indicating that the HIgG immobilized on the electrode surface was sufficient for specific conjugation of the HRP-anti-HIgG. On the other hand, at a low concentration range of HRP-anti-HIgG, the ECL quenching response sharply increased with the increasing HRP-anti-HIgG concentration in incubation solution. However, when the concentration of HRP-anti-HIgG was higher than 10 μg mL^{-1}, the ECL quenching slowly increased. Thus, 50 μg mL^{-1} HIgG was used for immunosensor preparation, and 10 μg mL^{-1} HRP-anti-HIgG in 20 μL incubation solution was used for immunoassay.

HIgG Detection with the Proposed Immunosensor. Competitive immunoassay was applied for the measurement of HIgG. Ten μL of HIgG standard solution at known concentration was mixed with 10 μL of 20 μg mL^{-1} HRP-anti-HIgG. The HIgG in the incubation solution competed with the immobilized HIgG on the immunosensor surface to bind the limited binding sites of the HRP-anti-HIgG to form the immunocomplex. In the presence of 0.1 mM HQ, the cyclic ECL curves of the GCE/QDs/chitosan-HIgG/HRP-anti-HIgG formed at respective concentrations of HIgG were shown in Figure 6. The ECL intensity decreased with the decreasing HIgG concentration in the incubation solution, which could be attributed to the increased impedance and the enzymatic reaction on electrode surface due to the conjugation of more enzyme-labeled antibody. The increased impedance lowered the reduction rate of dissolved oxygen, and thus inhibited the ECL reaction and decreased the ECL intensity. However, the contribution of impedance to the ECL quenching at low HIgG concentrations was slight when compared with that from the enzymatic cycle (Figure 7). In the absence of HQ, upon the immunoreaction the immunosensor could show a quenching effect of the increased impedance at HIgG concentrations higher than 0.5 μg mL^{-1} (Figure 7, curve a). Contrarily, in the presence of 0.1 mM HQ, the ECL intensity linearly decreased down to a HIgG concentration of 0.05 ng mL^{-1} (Figure 7, curve b). Moreover, the ECL emission at 0.5 μg mL^{-1} HIgG was also weaker than that in the absence of HQ due to the consumption of the self-produced H_2O_2. The linear concentration range for immunoassay of HIgG was from 0.05 ng mL^{-1} to 5 μg mL^{-1} with a limit of detection (LOD) of 0.01 ng mL^{-1} at S/N of 3 (Inset in Figure 6). The LOD was much lower than those of 3.75−1660 ng mL^{-1} for the reported competitive electrochemical immunosensors (Table 1),[46−52] though a competitive electrochemical immunoassay microdevice showed a LOD of 118 fg

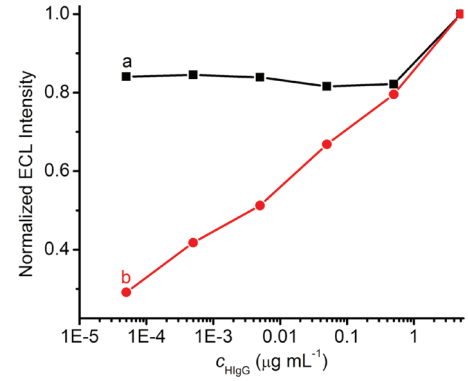

Figure 7. Plots of ECL intensity of immunosensor vs. HIgG concentration in absence (a) and presence (b) of 0.1 mM HQ in air-saturated pH 9.0 tris-HCl buffer containing 0.1 M KNO_3.

Table 1. Analytical Performances of the Reported Competitive Electrochemical Methods for IgG (in ng mL^{-1})

LOD	detection range	ref	LOD	detection range	ref
3.75	7.8−555	46	300	300−1500	50
1660	2000−5000	47	165	165−15000	51
1000	1000−6000	48		0−14000	52
7.0	7.0−140	49	1.18×10^{-4}	$1.18 \times 10^{-4} \sim 1.18$	53

(46) Campanella, L.; Lelo, D.; Martini, E.; Tomassetti, M. *Sensors* **2008**, *8*, 6727–6746.
(47) Sánchez, S.; Pumera, M.; Fàbregas, E. *Biosens. Bioelectron.* **2007**, *23*, 332–340.
(48) Ordóñez, S. S.; Fàbregas, E. *Biosens. Bioelectron.* **2007**, *22*, 965–972.
(49) Díaz-González, M.; Hernández-Santos, D.; González-García, M. B.; Costa-García, A. *Talanta* **2005**, *65*, 565–573.
(50) Zacco, E.; Pividori, M. I.; Llopis, X.; del Valle, M.; Alegret, S. *J. Immunol. Methods* **2004**, *286*, 35–46.
(51) Fernández-Sánchez, C.; Costa-García, A. *Anal. Chim. Acta* **1999**, *402*, 119–127.
(52) Santandreu, M.; Céspedes, F.; Alegret, S.; Martínez-Fàbregas, E. *Anal. Chem.* **1997**, *69*, 2080–2085.

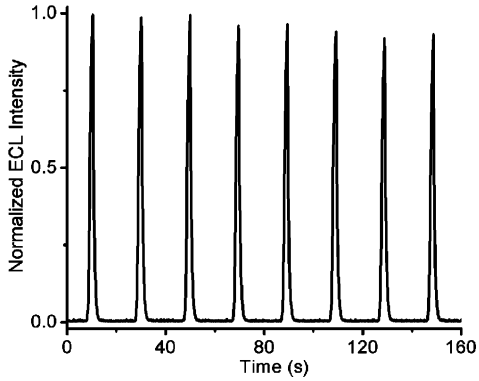

Figure 8. Continuous cyclic scans of GCE/QDs/chitosan-HIgG/HRP-anti-HIgG at 5 ng mL^{-1} of HIgG in air-saturated pH 9.0 tris-HCl buffer containing 0.1 M KNO_3 and 0.1 mM HQ. Scan rate: 0.1 V s^{-1}.

mL^{-1}.[53] The enzymatic amplification greatly increased the sensitivity and extended the detectable concentration range from 2 to 5 orders of magnitude.

Reproducibility and Precision of the Immunosensor. The relative standard deviation (RSD) for six parallel measurements with one GCE/QDs/chitosan-HIgG (intraassay) incubated with the incubation solution containing 5.0 ng mL^{-1} HIgG was 0.96%, indicating a good precision. The detection of 5.0 ng mL^{-1} HIgG with six GCE/QDs/chitosan-HIgG fabricated independently (interassay) showed a RSD of 5.05%, giving an acceptable fabrication reproducibility of the immunosensors. Eight measurements of ECL emission upon continuous cyclic scans of the GCE/QDs/chitosan-HIgG/HRP-anti-HIgG formed at 5.0 ng mL^{-1} HIgG showed coincident signal with RSD of 2.9% (Figure 8), indicating acceptable reliability and stability of the signal.

Analysis of Human Serum Samples. To evaluate the analytical reliability and application potential of the proposed method, the immunosensor was employed to detect IgG content in human serum samples. The assay results of clinical serum samples using the proposed method were compared with reference values obtained by commercial turbidimetric immunoassay. When the level of HIgG was over the calibration range, serum sample was appropriately diluted with 0.01 M pH 7.4 PBS prior to the assay. The results were listed in Table 2. Compared with the referred values, the relative errors were less than 3.48%, indicating acceptable accuracy.

(53) Dong, H.; Li, C. M.; Zhou, Q.; Sun, J. B.; Miao, J. M. *Biosens. Bioelectron.* **2006**, *22*, 621–626.

Table 2. Comparison of IgG Determinations in Human Serum Samples with the proposed Immunosensor and Turbidimetric Immunoassay (in ng mL^{-1})

serum sample no.	1[a]	1[b]	1[c]	2[a]	3[a]
proposed method	14.96	1584	1.52	12.86	10.56
turbidimetric immunoassay	15.50	1550	1.55	13.00	10.90
relative error (%)	3.48	2.19	1.94	1.08	3.12

[a] The serum samples were diluted at 1×10^6 times. [b] The serum samples were diluted at 1×10^4 times. [c] The serum samples were diluted at 1×10^7 times.

CONCLUSIONS

A sensitive competitive QD-based ECL immunosensor was designed by immobilizing DMSA-CdTe QDs and antigen on an electrode surface. The ECL emission could be generated in presence of the coreactant H_2O_2 self-produced from oxygen reduction during the cathodic scan. A simple enzymatic amplification strategy was proposed by combining the coreactant and the competitively conjugated HRP-labeled antibody. In presence of enzymatic substrate in the detection solution, the enzymatic amplification greatly increased the sensitivity and extended the detectable concentration range. The low-potential ECL emission and the self-produced coreactant made the immunoassay milder and more convenient. The immunosensor showed high sensitivity, wide linear range, good reproducibility and acceptable precision and accuracy. This work provided a new method for signal amplification and highly sensitive immunoassay. It would extend the application of QDs in ECL biosensing.

ACKNOWLEDGMENT

We gratefully acknowledge the National Key Technologies R & D Program of China (2009ZX10004-313), National Basic Research Program (2010CB732400), National Natural Science Foundation of China (20821063, 90713015, 20875044).

Received for review May 28, 2010. Accepted July 27, 2010.

AC1013942